Int. J. Electrochem. Sci., 10 **(2015)** 4718 - 4731

International Journal of
ELECTROCHEMICAL
SCIENCE
www.electrochemsci.org

Nanostructured Platform Based on Graphene-Polypyrrole Composite for Immunosensor Fabrication

Andreea Cernat, Mihaela Tertiș, Claudia Nicoleta Păpară, Ede Bodoki[*]*, Robert Săndulescu*

Analytical Chemistry Department, Faculty of Pharmacy, Iuliu Haţieganu University of Medicine and Pharmacy, 4 Pasteur St., 400349 Cluj-Napoca, Romania
[*]E-mail: bodokie@umfcluj.ro

Received: 2 March 2015 / *Accepted:* 8 April 2015 / *Published:* 28 April 2015

The entrapment of functionalized graphene, as filler, in polymeric conductive layers, such as polypyrrole (PPy), improves their engineering features. The objective was the association of graphene-PPy composite with nanosphere lithography generating hybrid polystyrene-graphene-PPy patterned platforms, seeking a further enhancement of their characteristics: an improved mechanical stability and electron transfer rate, combined with an increase of the active surface area. Additionally, the substrate was modified with *N*-hydroxysuccinimide activated carboxylic functional groups, for the controlled immobilization of Antiparacetamol antibody in order to elaborate an immunosensor for paracetamol detection. The behavior of the nanostructured hybrid platform was tested by imagistic, impedimetric and electrochemical quartz crystal microbalance experiments, which proved the successful patterning of the composite material and the biomolecule's immobilization. The sensor allowed the specific detection of paracetamol on a linear range of 0.1 to 25 µM on the unstructured platform. The analytical signal was improved on the patterned material in comparison with the non-structured one, proving the superior nature of the structured surface.

Keywords: graphene, polypyrrole, nanosphere lithography, paracetamol, immunosensor

1. INTRODUCTION

The continuous development of materials is pursued in all major fields of technology including the biomedical one due to the increasing demands on the market. Their chemical, mechanical and electrochemical properties represent the key factor in the fabrication of new and improved materials and it can be achieved by different techniques such as including nanoparticles, nanotubes, graphene, increasing the active surface area by nanosphere lithography (NSL) or by combining two or more materials depending on the demands [1-3].

The biosensors' development is one of the most efficient ways to achieve a high specificity and selectivity towards an analyte, short response time and low analysis cost [4, 5]. They can be used in real-time analysis and they have a wide range of applications in pharmaceutical analysis, medical diagnosis, clinical analysis, environmental assays, food safety and industrial processes [6, 7]. The electrochemical biosensors based on nanomaterials such as metal nanoparticles, carbon nanotubes and graphene have been intensively investigated, due to their chemical and physical features [8].

Graphene consists in a transparent single layer of sp^2 hybridized carbon, atoms, arranged in a "honeycomb" pattern with excellent electric and mechanical properties, due to its high specific surface area and double bond conjugation [9-11]. As a consequence, graphene have gained an increasing attention in the field of new materials industry being involved in wide range of applications, such as: electroanalysis, sensors, drug delivery, tissue engineering. Graphene are very promising fillers in the engineering of conductive polymer nanocomposites, providing a higher available surface for biomolecule immobilization [12-16].

Polymer nanocomposites combine the polymeric matrix, that can be easily functionalized and controlled, with a wide variety of molecules that can act as fillers [17]. Based on the type of interactions between the matrix and the surface of graphene, different structures may be generated, suitable for various applications in the development of nanoplatforms [2]. The entrapment of functionalized graphene within polymeric films, increased the interfacial interactions at a molecular level and improved the material strength.

Due to its good chemical and thermal stability under various experimental conditions and its biocompatibility, PPy has been a subject of extensive investigation during the last four decades being widely used in sensor and biosensor development [18-22]. The nanocomposite materials obtained by the inclusion of activated graphene within a PPy layer led to highly stable films, with a good mechanical strength, improved electrical conductivity and a larger active surface area [3, 23]. The overoxidation of the PPy layer at positive potentials, generally used in order to reduce its electroactivity in the detection range of the analyte, determined the polymer degradation and loss of conductivity [24, 25]. The incorporation of activated graphene oxide sheets overcomes this drawback, by increasing the active surface area available for the immobilization of the biorecognition element and facilitating the electronic transfer between the analyte and the transducer.

The nanostructuration by NSL of polymers generates a variety of morphologies with particular properties in a simple and quick route, producing well-ordered structures, with increased active surface area, does not require any special equipment, and it can be applied at laboratory scale with low costs [26, 27].

The development of nanostructured graphene-PPy composite material with improved surface properties, as platform for immunosensor fabrication was achieved by using NSL. The antiacetaminophen antibody (ApAb) was immobilized as a biorecognition element onto the nanostructured hybrid surface and its immobilization was indirectly proved by paracetamol's detection.

2. MATERIALS AND METHODS

2.1. Chemical and materials

Disodium hydrogen phosphate, sodium dihydrogen phosphate, potassium ferrocyanide ($K_4[Fe(CN)_6]$), potassium ferricyanide ($K_3[Fe(CN)_6]$) and paracetamol were purchased from Merck (Whitehouse Station, NJ, USA). Monodisperse carboxylate-modified polystyrene (PS) spheres with diameters of 900 nm (10 wt.% suspensions in water), pyyrole (Py), lithium perchlorate and tetrahydrofuran were obtained from Sigma-Aldrich. Sheep polyclonal IgG antiacetaminophen antibody (ApAb) in serum (0.5 mg ml^{-1}) was purchased from AbD Serotec (Bio-Rad Laboratories, Puchheim, Germany. 1-Ethyl-3-(3-dimethylaminopropyl) carbodiimide hydrochloride (EDC) was purchased Calbiochem (Canada) and *N*-hydroxysuccinimide (NHS) from Alfa Aesar (Kalsruhe, Germany).

The functionalized graphene synthesis' was initiated by suspending 0.10 g graphene oxide in 10 ml of 400 μM EDC and 100 μM NHS ultrapure water [28]. The suspension was mixed 4 hours at room temperature and the NHS modified graphene oxide was separated by centrifugation and washed with ultrapure water for the removal of residual NHS and EDC. The solid product was dried at 45° C, suspended in ultrapure water by 30 min of sonication and left at room temperature. The concentration used for the preparation of the graphene layer was 0.5 mg ml^{-1}.

All the solutions were prepared using Milli-Q grade water. The 0.02 M phosphate buffer saline (PBS) solution was prepared with Na_2HPO_4, KH_2PO_4 and NaCl at pH 7.4.

2.2. Apparatus and characterization methods

Electrochemical studies were performed using a three electrode cell with an Ag/AgCl wire as a reference electrode and a platinum iridium doped electrode as counter electrode, both purchased from eDAQ, Australia. The working glassy carbon electrodes (GCE) (4 mm diameter) purchased from BASi (USA) were polished with alumina slurry (0.05 μm) prior to use.

Electrochemical experiments were performed using a Quadstat potentiostat (eDAQ, Australia). The polymerization of the Py and the film overoxidation were done by cyclic voltammetry in aqueous 5 mM monomer solutions using as supporting electrolyte lithium perchlorate and KPF_6. The signal after the incubation with several paracetamol concentrations was investigated by square wave voltammetry measurements in a 0.1 M KPF_6 solution, between 0 and 0.8 V vs Ag/AgCl, at a scan rate of 0.05 V s^{-1}, 25 mV pulse amplitude and 10 Hz pulse frequency.

The new hybrid surfaces were studied by electrochemical impedance spectroscopy (EIS) and electrochemical quartz crystal microbalance (EQCM) modules available on the Autolab PGSTAT100 potentiostat (Metrohm/EcoChemie Netherlands). The EIS experiments were performed after each modification step of both unstructured and structured hybrid platforms. The measurements were carried out in a 10 mM $[Fe(CN)_6]^{3-/4-}$ solution in PBS (0.02 M, pH 7.4) as electronic shuttle. The impedance was measured in a frequency range of 10 mHz to 100 KHz at open circuit potential. For the EQCM protocol, the Au coated quartz crystal electrodes (5.1 mm diameter) were washed with a *piranha* solution, containing H_2SO_4 and 30% H_2O_2 in a 3:1 combination ratio and then the crystal was

rinsed with ultrapure water, ethanol and dried in a N_2 current. The recordings were performed in ultrapure water after the oscillation frequency stabilization.

The hybrid structured platforms were also characterized by microscopy and Raman spectroscopy using optically transparent PEDOT (Poly(3,4-ethylenedioxythiophene)) screen-printed electrodes (DropSens, Spain) in order to avoid the superposition of graphene signal with the one of GCE surface. These disposable electrodes are made in a plastic substrate, with a PEDOT working electrode, a carbon counter electrode and a silver pseudoreference electrode. The potential range used for the PPy polymerization was slightly modified between -0.7 V and 0.9 V. Raman spectra were obtained on a confocal Raman microscope (WITec Alpha 300R), by using a 0.9 NA objective for illumination and collection, and a 532 nm laser as excitation source. The spectral range up to 3600 cm^{-1} was recorded in a single spectrum with a resolution of ~3 cm^{-1}.

2.3. Immunosensor fabrication

2.3.1. The generation of the unstructured hybrid platform

The activated graphene was deposited (10 µl 0.5% (w/v)) on the GCE surface by the drop coating method and it was allowed to dry at 45 ºC. The process was repeated 10 times in order to generate the graphene layer and the surface was rinsed with 0.02 M PBS.

The 5 mM Py polymerization was performed in a 0.1 M lithium perchlorate solution by scanning five times the potential between -0.8 V and 0.8 V vs Ag/AgCl, at a scan rate of 0.1 V s^{-1}. The PPy film was overoxidized in 0.1 M KPF_6 solution between -0.2 V and 1.2 V vs Ag/AgCl at 0.1V s^{-1}.

The modified electrode was rinsed with 2 ml of 0.02 M PBS.

2.3.2. The generation of the structured hybrid platform

The PS template was fabricated as follows [1, 29]: The suspension of PS spheres (900 nm diameter) was diluted with ethanol to 0.5 wt.% and a volume of 3 µL was spread over the GC surface and allowed to dry at room temperature for 10 minutes.

The activated graphene was deposited (10 µl 0.5% (w/v)) on the PS template surface by the drop coating method and it was allowed to dry at 45 ºC. The process was repeated 4 times.

Py polymerization and its overoxidation were performed as presented before. The PS template was removed by soaking the electrodes for 15 hours in tetrahydrofuran. The modified electrode was rinsed with ethanol and then with 2 ml of 0.02 M PBS.

2.4. The immobilization of ApAb

A 5 µl drop of ApAb solution was incubated on the surface of the PPy modified GCE for 15 minutes at room temperature and the functionalized electrodes were rinsed with 0.02 M PBS solution. The activated carboxyl groups of graphene, that did not react with the amino groups of the ApAb, were

blocked by the deposition of 20 µl of 5% (m/v) BSA solution on top of the hybrid platform followed by 20 minutes incubation. The last step was the incubation of the immunosensors for 15 minutes with 10 µl of aqueous solution of paracetamol in different concentrations. After each incubation step, the electrodes were rinsed with 2 ml of 0.02 M PBS, in order to remove the unbound compounds.

3. RESULTS AND DISCUSSION

The immobilization of the ApAb was made with graphene carboxylic groups that were activated by the coupling reaction with NHS/EDC, which is one of the most widely used crosslinking methods in the biomaterials field. The reaction was catalyzed by EDC, which couples NHS to carboxyl, forming an NHS reactive ester, allowing the efficient conjugation to primary amines at physiological pH. Therefore, the immobilization of the ApAb was performed by amidic covalent bonds between the activated carboxyl groups of graphene and the amino functions of the biocompound. This controlled immobilization method ensured the stability of the biomolecule and the orientation of its active center.

The deposition of the graphene onto the working electrode surface was performed by the layer by layer method, that proved to be an efficient fabrication for strong and thin films. This technique generated highly ordered and uniform structures. The immobilization of the graphene sheets on the GCE working surface involves electrostatic bonds, assuring the stability of the layers [2, 17]**.**

The thickness of the graphene layer was adapted depending on the optical and impedimetric studies for both configurations. Thus, for the unstructured platform were deposited 10 layers, according to our previously published study [28]. For the optimal thickness of the structured material only 4 graphene layers were deposited, because the increasing in the number of layers, in the presence of PS beads, determined a decrease in the electron transfer rate. In both cases, PPy was electropolymerized on top of the graphene layer in order to generate a hybrid PS-graphene-PPy surface with activated carboxyl groups available for biomolecule coupling, as showed in Fig.1.

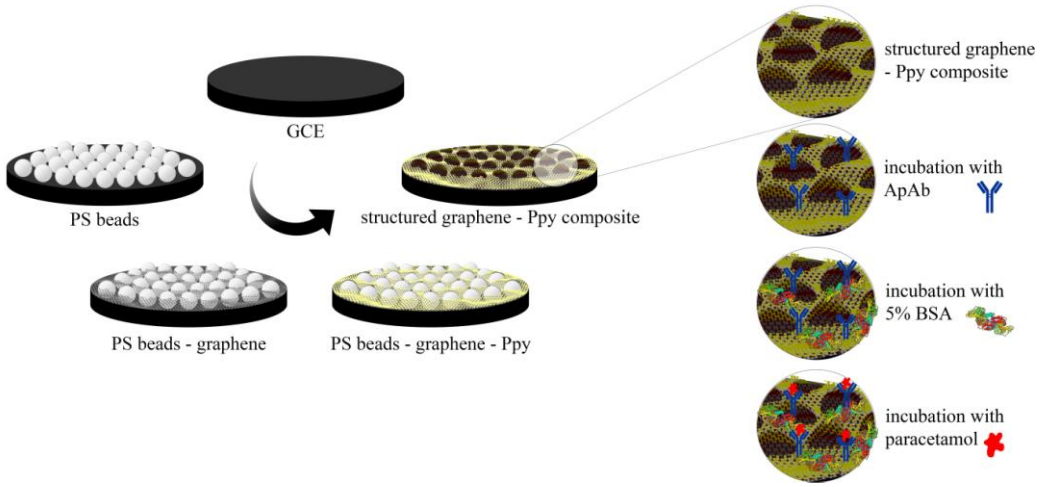

Figure 1. The development of the structured platform and the immunosensor fabrication

3.1. The generation of the hybrid platform

In Fig. 2A, it can be observed that the intensity of the oxidation system at 0 V increases proportionally with the number of cycles and corresponds to the electroactivity of the steadily growing PPy's backbone. The intensity of the signal was increased for the configuration with activated graphene, enhancing the PPy deposition by an increase of the active surface area of the electrode after the deposition of the graphene layers (Fig. 2B). As previously described in literature, the porous graphene assembly has a 3D structure, allowing the exposure of the graphene sheets to the electrolyte and providing open channels for the transportation of the electrolyte, ensuring the electron transfer between the immobilized molecule and the surface of the electrode [2]**.**

For the configuration where the 900 nm PS beads were deposited onto the GCE, followed by the deposition of graphene, the intensity of the current corresponding to the Py polymerization was diminished due to the blocking effect generated by the template at the working surface, as it can be observed in Fig. 2C.

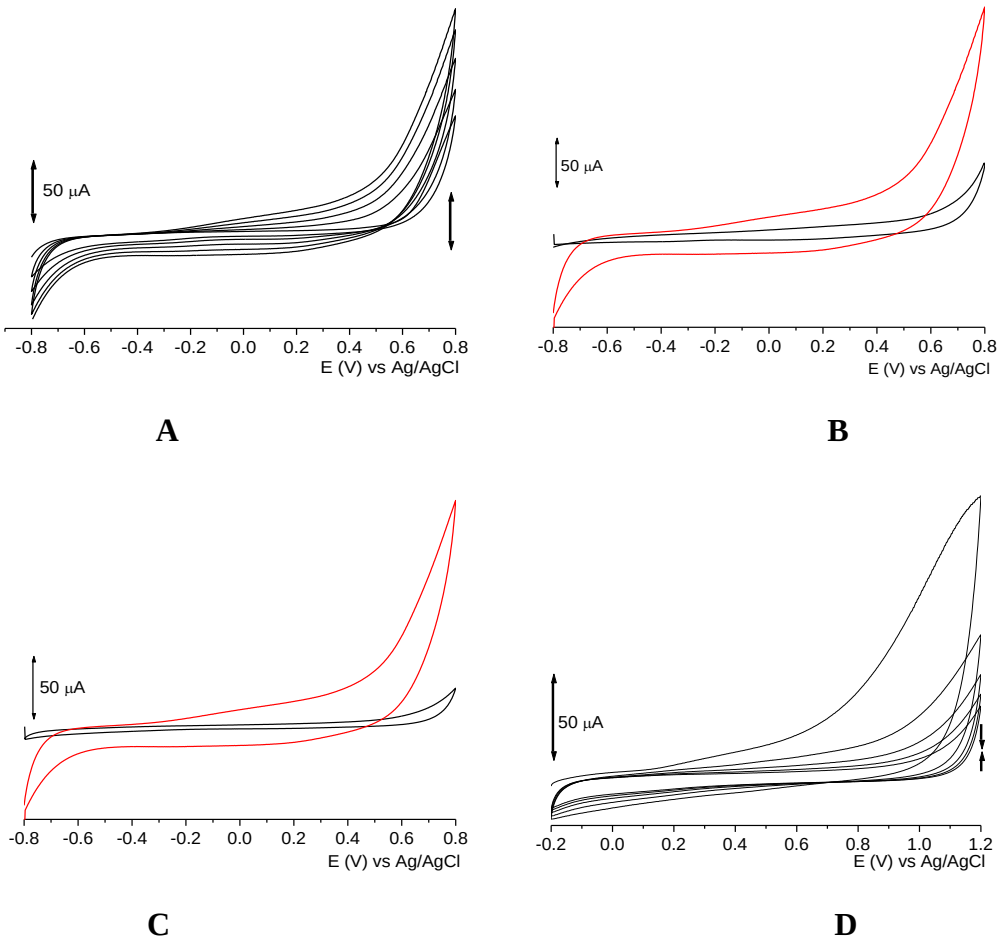

Figure 2. (A) The electrodeposition of PPy on the graphene layer; 5th cycle of the polymerization for (B) PPy on the bare GC electrode (black line) and on the graphene layer (red line), (C) PPy on the PS beads-graphene-layer (black line) and on the graphene layer (red line) (-0.8 to 0.8 V vs Ag/AgCl, 0.5 Vs^{-1}); (D) Overoxidation of PPy on the PS-graphene substrate (-0.2 to 1.2 V vs Ag/AgCl, 0.1 Vs^{-1})

For both configurations the one with and without the PS template, the PPy's electroactivity in the potential range of paracetamol detection was reduced. The film was overoxidized by cyclic voltammetry in a 0.1 M KPF_6 aqueous solution by performing 5 scans between -0.2 V and 1.2 V vs. Ag/AgCl. Proportionally with the number of potential scans performed, the overoxidation of the PPy film has led to a steady state baseline with low background current, available for the subsequent detection of the target molecule, as shown on Fig. 2D. At more anodic potentials the chemical structure of the polymer changes corresponding to the film's redox couple diminution [24]**.** The loss of conductivity and the deterioration of the polymeric matrix, as a consequence of the overoxidation, were compensated by the incorporation of graphene, that led to an increase of the electron transfer between the target analyte (paracetamol) and the transducer.

3.2. Electrochemical impedance spectroscopy

EIS measurements study the interfacial charge-transfer phenomena and they were carried out in order to characterize the modifications performed on the electrode's surface. This technique allows the measurement of the electrochemical response, including the rate constant of the electrochemical reaction, the double-layer capacitance and the diffusion coefficient of the redox species [30]. The Nyquist plot is the representation of imaginary impedance (-Z'') versus real impedance (Z') as a function of decreasing frequency. It offers important information depending on the nature of the electrode reaction. If the rate-determining electrode reaction step is the electron transfer reaction of the probe, the Nyquist plot is represented by a semicircle and if diffusion of the process is rate determining, a linear Nyquist plot is obtained [31].

The electron transfer properties of the new hybrid surfaces were evaluated step by step by EIS measurements performed in a 10 mM $[Fe(CN)_6]^{3-/4-}$ solution used as a redox probe. The Nyquist plots indicated modifications in charge transfer resistance (R_{ct}) depending on the nature of the modifier. As it can be observed from Fig. 2B, the activated graphene layer increased the electron transfer in comparison with the unmodified electrode. The R_{ct} of the graphene layer increased from 0.545 kΩ to 14.9 kΩ, when the PS template is added into the system, reducing the electron transfer rate, as expected due to the insulating effect of the PS. After the polymerization of Py and the overoxidation of Ppy a further decrease of electron transfer (259 kΩ) can be observed caused by the polymeric film deposited on the PS and graphene layer. The signal was partially regained after the removal of the PS beads by dissolution in tetrahydrofuran (25.8 kΩ). The removal of the template reduced the value of R_{ct}, by facilitating the access to the graphene layer or to the bare electrode surface. This behavior confirms that the nanostructuration by NSL improved the electroactive properties of the hybrid surfaces by increasing the active surface area. The variation of R_{ct} depending on the type of modification is presented in Fig. 2.

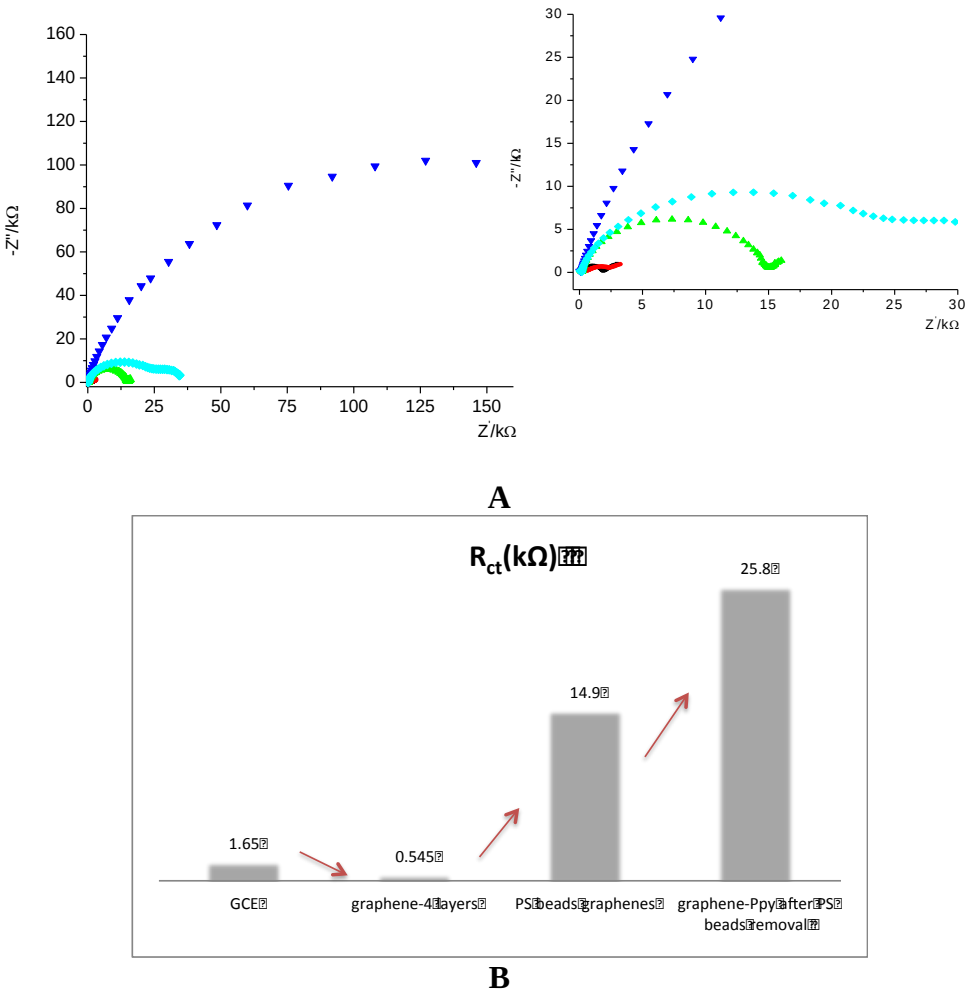

Figure 3. EIS measurements performed at each step of the fabrication of the PS-graphene-PPy hybrid surface: (A) bare GCE (black), graphene-4 layers (red), PS beads-graphene layer (green), PS beads-graphene layer-PPy (dark blue), graphene layer-PPy after PS beads removal (light blue), Inset: detail of A (b) The evolution of R_{ct} depending on the modification step

3.3. Structural characterization of the composite material

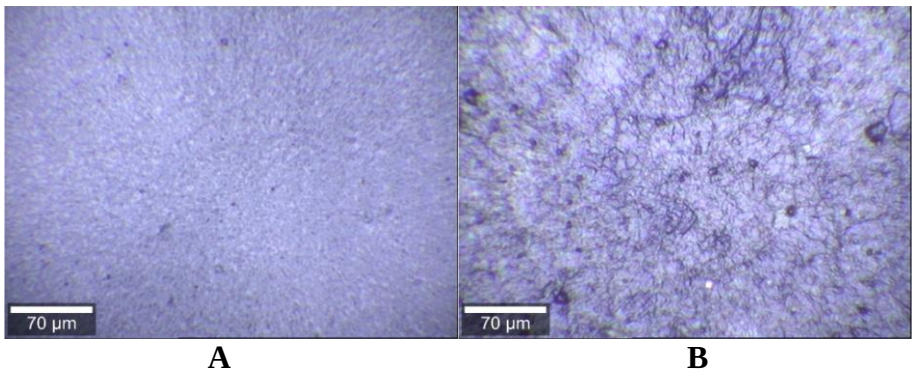

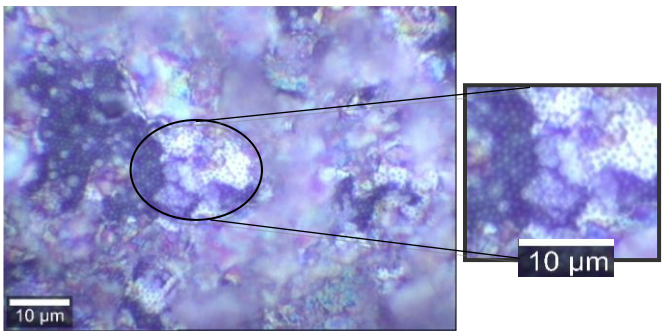

C

Figure 4. Optical microscopy images performed on the (A) PPy layer, (B) graphene-PPy composite, (C) PS-graphene-PPy hybrid surface

Optical microscopy was used in order to confirm each step in the generation of the structured hybrid material performed at the GCE surface. As it can be seen from Fig. 4A and B, the graphene-PPy layer has a rougher surface with micrometric scale bulges in comparison with the PPy layer. The presence of the template generates another type of structure, in which nanospheres arranged in a hexagonally close-packed pattern are to be observed on the substrate (Fig. 4C). After the solvent evaporation the mechanism for the generation of the PS template was represented by the capillary forces that determined the nanospheres to be drawn together and ″crystallize″ [32]. After this step, the graphene layer was grown in-between the template, followed by the PPy deposition.

The results were confirmed by Raman spectroscopy performed on the composite surfaces. In the Raman spectra of the activated graphene, with NHS covalently attached were observed three characteristic bands (Figure 5): two strong bands close to 1353 cm^{-1} (D band) and 1598 cm^{-1} (G band) and a weaker one in the 2500–3000 cm^{-1} region (2D band), in accordance with previously published data [33]. The same bands can be also distinguished in the configuration with graphene and PPy. In this case the signal was also compared with the one obtained on a PPy layer, as presented in Fig. 5. The characteristic bands of the PPy are visible at 1050 cm^{-1} [34, 35]. In the case of the hybrid surface, the PPy bands are clearly present, although they are less visible due to the higher intensity of the signal generated by the graphene.

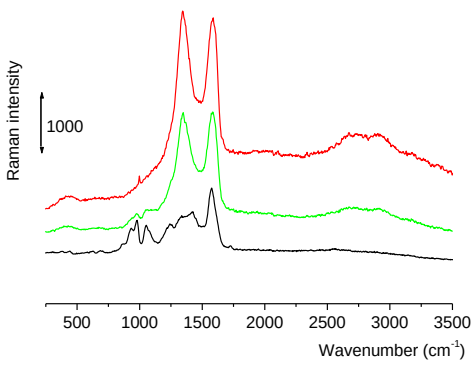

Figure 5. Raman spectra of the graphene layer (red line), PPy film (black line) and on the graphene-PPy composite (green line)

3.4. EQCM studies

EQCM has been recently used for studying the steps involved in the development of platforms for immunosensors and also for the evaluation of interactions between antibodies and antigens [36]. In this case, the transducer is represented by an oscillating quartz crystal whose resonance frequency depends on the change in the mass according to the Sauerbrey equation [28, 37, 38]**.**

The fabrication of the modified graphene-PPy composite was studied by registering the variation of the oscillation frequency after each step of the protocol (deposition of graphene, PPy layer electrosynthesis and overoxidation, incubation with the ApAb and blocking with BSA).

Based on the Sauerbrey equation, the relationship between the resonant oscillation frequency can be correlated with the change in mass deposited on the piezoelectric crystal: $\Delta f = - C_f \cdot \Delta m$, where C_f represents the sensitivity factor equivalent with 0.0815 Hz $\cdot$ ng^{-1} $\cdot$ cm^{-2} for the 6 MHz crystal from Methrom Autolab (Netherlands). Knowing the fact that the Au QCM crystal has an active surface of 0.196 cm^2, the mass deposited on EQCM crystal can be determined using the equation mentioned above.

In Fig 6, it can be observed the decrease in the frequency after the deposition of the graphene-PPy composite, suggesting the deposition of the film on the Au surface. After this step, the incubation with the ApAb led to a further decrease of the oscillation frequency, suggesting that the biomolecule was immobilized on the substrate by a covalent bond between the activated carboxylic groups of the polymeric platform and the amino groups of the ApAb. By correlating the variation in the oscillation frequency on the quartz crystal with the mass it was estimated that in the first step, corresponding to the graphene-polymer composite construction, 20.19 µg were deposited. After the incubation with 5 µg ApAb, the recorded mass increase was of 2.65 µg, proving the coupling of approximately 50% of the biocompound. The free activated carboxylic groups were then blocked with a 5% BSA solution in order to prevent the non-specific adsorption of the target molecule, leading to the accumulation of 4.62 µg albumin.

The experiments were repeated on 2 different EQCM gold crystals and the results represent the mean of two determinations.

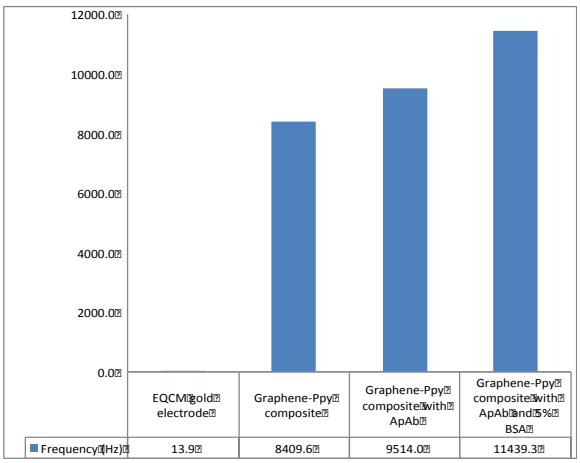

Figure 6. Variation of the EQCM resonant frequency depending on the modification step

3.5. Immunosensor development

After the fabrication of the unstructured and structured graphene-PPy hybrid platform, its properties were tested by incubating the ApAb, that can specifically bind paracetamol, a stable and electrochemically active model molecule (Fig 1). The immobilization protocol was optimized in terms of incubation time and concentrations according to our previous work [28].

The successful immobilization of the antibody on the composite layer was indirectly proved by the detection of paracetamol, which was incubated in different concentrations on the hybrid material.

Prior to this step, the activated carboxylic groups of graphene were blocked by incubation with a 5% BSA solution. This step is critical in the development of immunosensors, the non-specific adsorption of the target analyte on the sensing platforms being a well-known disadvantage. The BSA molecules also form a covalent amidic bond with the carboxyl groups preventing other molecules with amino functions to react with the graphene layer, but partly it may also be physisorbed onto the substrate.

The increase of the oxidation current of paracetamol was proportional with the incubated concentrations in the range of 0.1 to 25 μM (Fig. 7). At higher concentrations the binding capacity of ApAb was reduced because the active centers could be saturated or the antibody denatured.

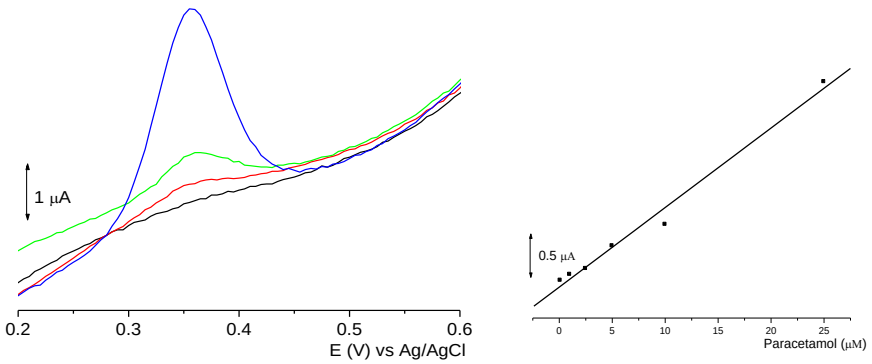

Figure 7. Variation of the intensity of the current following the incubation of different concentrations of paracetamol on the graphene-PPy platform (ApAb was incubated for 60 minutes, 5% BSA for 20 minutes and paracetamol 15 minutes) 1 μM (black line), 5 μM (red line), 10 μM (green line), 50 μM (blue line). Inset: Calibration curve for paracetamol on the unstructured surface

After the fabrication of the structured PS-graphene-PPy platform, the ApAb was immobilized in the same conditions as depicted in Fig. 7. After the incubation of paracetamol on the patterned surface, a five times fold increase of the signal was observed compared with the one obtained on the unstructured surface. As expected, the structuration of the graphene-PPy composite via NSL, using a PS template with 900 nm diameter spheres, determined the enhancement of the active surface area [1, 26, 39].

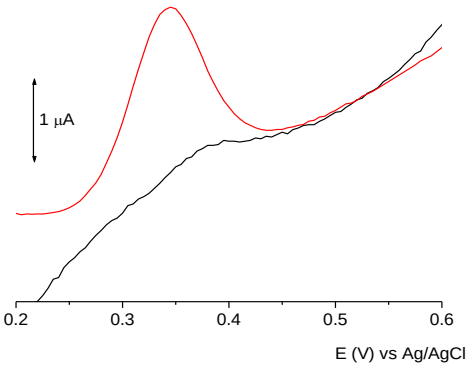

Figure 8. Variation of the intensity of the current following the incubation of 5 µM paracetamol solution with the unstructured (black line) and structured (red line) graphene-PPy platform (ApAb was incubated for 60 minutes, 5% BSA for 20 minutes and paracetamol 15 minutes)

The patterning generated an augmentation of the number of carboxylic functions available for the immobilization of the biorecognition element. In consequence, this led to a higher number of ApAb entities coupled by amidic bonds to the structured graphene-PPy platform and to an increase of the signal corresponding to the electrochemically oxidation of paracetamol.

4. CONCLUSIONS

The fabrication of a hybrid composite graphene-PPy platform structured by NSL was proven, which was used for the immobilization of ApAb as biorecognition element. The electrochemical immunosensor was tested for paracetamol detection. The five-fold improvement of electrochemical signal recorded on the structured surface is suggesting that the patterning of the composite layer led to the immobilization of a higher amount of antibody. Such nanopatterning strategies along with the facile and controlled immobilization of bioreceptors on the composite grapheme-PPy platform may be further exploited in the development of other immune- and aptasensors in the detection of relevant biomarkers.

ACKNOWLEDGEMENTS
The authors are thankful to dr. Cosmin Farcău from "Babeș-Bolyai" University, Faculty of Physics, Institute for Interdisciplinary Research in Bio-Nano-Sciences for the Raman and optical microscopy experiments. This paper was published under the frame of European Social Found, Human Resources Development Operational Programme 2007-2013, project no. POSDRU/159/1.5/S/136893. The authors are also thankful for the financial support of University of Medicine and Pharmacy "Iuliu Haţieganu" Cluj-Napoca by the research grant no. 1491/5/28.01.2014.

References

1. A. Cernat, S. Griveau, P. Martin, J.C. Lacroix, C. Farcau, R. Sandulescu and F. Bedioui., *Electrochem. Commun.*, 23 (2012) 141;

2. G. Mittal, V. Dhand, K. Y. Rhee, S.-J. Park and W. R. Lee, *J. Ind. Eng. Chem.*, 21 (2015) 11;
3. K. Xue, S. Zhou, H. Shi, X. Feng, H. Xin and W. Song, *Sensor. Actuat. B-Chem.*, 203 (2014) 412;
4. Ö. Türkarslan, A.E. Böyükbayram, L. Toppare, *Synthetic Met.*, 160 (2010) 808;
5. A. Sassolas, L.J. Blum and B.D. Leca-Bouvier, *Biotech. Adv.*, 30 (2012) 489;
6. M. Singh, P.K. Kathuroju and N. Jampana, *Sensor. Actuat. B-Chem.*, 143 (2009) 430;
7. E. Horozova, T. Dodevska and N. Dimcheva, *Bioelectrochemistry*, 74 (2009) 260;
8. Y. Xiao and C.M. Li, *Electroanal.*, 20 (2008) 648;
9. S. Sahoo, G. Karthikeyan, G. Ch. Nayak and C. Kumar Das, *Synthetic Met.*, 161 (2011) 1713;
10. R. Yamuna, S. Ramakrishnan, K. Dhara, R. Devi, N.K. Kothurkar, E. Kirubha and P.K. Palanisamy, *J. Nanopart. Res.*, 15 (2013) 1399;
11. Y. Liu, H. Wang, J. Zhou, L. Bian, E. Zhu, J. Hai, J. Tang and W. Tang, *Electrochim. Acta*, 112 (2013) 44;
12. L. Zhao, F. Zhao and B. Zeng, *Electrochim. Acta*, 115 (2014) 247;
13. F. Wang, L. Zhu and J. Zhang, *Sensor. Actuat. B-Chem.*, 192 (2014) 642;
14. R. Justin and B. Chen, *Carbohydr. Polym*, 103 (2014) 70;
15. H.C. Tian, J.Q. Liu, D.X. Wei, X.Y. Kang, C. Zhang, J.C. Du, B. Yang, X. Chen, H.Y. Zhu, Y.N. Li and C.S. Yang, *Biomater*., 35 (2014) 2120;
16. D. Nandi, S. Nandi, P.K. Pal, A.K. Ghosh, A. De and U.C. Ghosh, *Appl. Surf. Sci.*, 293 (2014) 90;
17. K. Hu, D.D. Kulkarni, I. Choi and V.V. Tsukruk, *Prog. Polym. Sci*, 39 (2014) 1934;
18. M. Deepa and S. Ahmad, *Eur. Polym. J.*, 44 (2008) 3288;
19. D. Nandi, A.K. Ghosh, K. Gupta, A. De, P. Sen, A. Duttachowdhury and U.C. Ghosh, *Mater. Res. Bull.*, 47 (2012) 2095;
20. H. Li, Q. Zhou, P. Audebert, F. Miomondre, C. Allain, F. Yang and J. Tang, *J. Electroanal. Chem.*, 668 (2012) 26;
21. A. Ramanaviciene, A. Kausaite-Minkstimiene, Y. Oztekin, G. Carac, J. Voronovic, N. German and A. Ramanavicius, *Microchim. Acta*, 175 (2011) 79;
22. R. Pertines, R. Ponnapati, M.J.Felipe and R. Advincula, *Biosens. Bioelectron.*, 26 (2011) 2766;
23. C. Bora and S.K. Dolui, *Polymer*, 53 (2012) 923;
24. S. Cosnier and A. Karyakin, *Electropolymerization: Concepts, Materials and Applications*, Wiley (2010);
25. P. S. Sharma, A. Pietrzyk-Le, F. D'Souza and W. Kutner, *Anal. Bioanal. Chem.*, 402 (2012) 3177;
26. A. Cernat, A. Le Goff, M. Holzinger, R. Sandulescu and S. Cosnier, *Anal. Bioanal. Chem.*, 406 (2014) 1141;
27. A. Cernat, E. Bodoki, C. Farcau, S. Astilean, S. Griveau, F. Bedioui F and R. Săndulescu, *J. Nanosci. Nanotechno.*, 15 (2015) 3359;
28. M. Tertiș, O. Hosu, L. Fritea, C. Farcau, A. Cernat, R. Sandulescu and C. Cristea, *Electroanal., accepted* DOI: 10.1002/elan.201400583;
29. L. Santos, P. Martin, J. Ghilane, P.-C. Lacaze, H. Randriamahazaka, L.M. Abrantes and J.C. Lacroix, *Electrochem. Commun.*, 12 (2010) 872;
30. M. Tertiș, A. Florea, B. Feier, I. O. Marian, L. Silaghi-Dumitrescu, A. Cristea, R. Săndulescu and C. Cristea, *J. Nanosci. Nanotechnol.*, 15 (2015) 3385;
31. X. Liu, P. A. Duckworth and D. K.Y. Wong, *Biosens. Bioelectron.*, 25 (2010), 1467;
32. C. Acikgoz, M.A. Hempenius, J. Huskens and G.J.Vancso, *Eur. Polym. J.*, 47 (2011) 2033;
33. K. Bustos-Ramirez, A.L. Martinez-Hernandez, G. Martinez-Barrera, M. De Icaza, V.M. Castano and C. Velasco-Santos, *Materials*, 6 (2013) 911;
34. D. K. Singh, S. K. Srivastava, A. K. Ojha and B.P. Asthana, *Spectrochim. Acta A*, 71 (2008) 823;
35. S. J. Vigmond, V. Ghaemmaghami and M. Thompson, *Can. J. Chem*, 73 (1995) 1711;
36. X. Pei, B. Zhang, J. Tang, B. Liu, W. Lai and D. Tang, *Anal. Chim. Acta*, 758 (2013) 1;
37. R. Chauhan, P. R. Solanki, J. Singh, I. Mukherjee, T. Basu and B.D. Malhotra, *Food Control*, 52 (2015) 60;

38. G. Sauerbrey, *Z. Phys.*, 55 (1959) 206;
39. A. Cernat, S. Griveau, C. Richard, F. Bedioui and R. Săndulescu, *Electroanal.*, 25(2013) 1369.

© 2015 The Authors. Published by ESG (www.electrochemsci.org). This article is an open access article distributed under the terms and conditions of the Creative Commons Attribution license (http://creativecommons.org/licenses/by/4.0/).